ISSN 1063-7737, Astronomy Letters, 2011, Vol. 37, No. 1, pp. 1–10. © Pleiades Publishing, Inc., 2011.
Original Russian Text © O.K. Sil'chenko, I.V. Chilingarian, 2011, published in Pis'ma v Astronomicheskiĭ Zhurnal, 2011, Vol. 37, No. 1, pp. 3–12.

Star Formation History at the Centers of Lenticular Galaxies with Bars and Purely Exponential Outer Disks from SAURON Data

O. K. Sil'chenko[1*] and I. V. Chilingarian[1,2]

[1] *Sternberg Astronomical Institute, Universitetskii pr. 13, Moscow, 119992 Russia*
[2] *Strasbourg Observatory, CNRS UMR 7550, France*

Received February 8, 2010

Abstract—We have investigated the stellar population properties in the central regions of a sample of lenticular galaxies with bars and single-exponential outer stellar disks using the data from the SAURON integral-field spectrograph retrieved from the open Isaac Newton Group Archive. We have detected chemically decoupled compact stellar nuclei with a metallicity twice that of the stellar population in the bulges in seven of the eight galaxies. A starburst is currently going on at the center of the eighth galaxy and we have failed to determine the stellar population properties from its spectrum. The mean stellar ages in the chemically decoupled nuclei found range from 1 to 11 Gyr. The scenarios for the origin of both decoupled nuclei and lenticular galaxies as a whole are discussed.

DOI: 10.1134/S1063773710101019

Keywords: *galactic nuclei, galactic structure, galactic evolution.*

INTRODUCTION

Almost at the dawn of galactic research, it was noticed that the radial surface brightness distribution in galactic disks has a universal shape—the surface brightness falls exponentially along the radius (de Vaucouleurs 1959; Freeman 1970). However, the origin and nature of this universality still remain unclear. Public opinion is inclined to believe that this property is primordial, i.e., it is tied up with the initial conditions at the time of galaxy formation: cooling down in the dark halo on a time scale of ∼1 Gyr, the gas settles into the disk with an already exponential surface density profile (see, e.g., Churches et al. 2001) and, subsequently, the forming stars continue to "follow" this law. However, there were also theoretical works with a justification for an alternative viewpoint—that an exponential surface density profile is established in the stellar disk for any initial gas distribution in the process of secular evolution if the star formation time scale is of the order of the viscous time scale in the gaseous disk (Lin and Pringle 1987; Clarke 1989; Slyz et al. 2002); so far, the proponents of this approach have been in the minority, though.

However, as the accuracy and depth of galactic surface photometry increase, it has been ascertained that the typical shape of the disk surface brightness profile is not at all exponential but broken exponential (see, e.g., Pohlen and Trujillo 2006). Most galactic disks exhibit a double exponential: at some radius, the profile breaks or goes to zero with a shorter scale length ("truncated" disks) or continues outward with a longer scale ("antitruncated" or two-tiered disks). There are not so many purely exponential disks that retain a single characteristic scale of brightness decline along their whole length: for example, according to the SDSS statistics, there are only 10% of them among the late-type galaxies (Pohlen and Trujillo 2006). Recently, Erwin et al. (2008) published the statistics of the shapes of the radial surface brightness profiles for early-type barred disk galaxies. Only about a quarter of all galaxies with purely exponential brightness profiles of their outer stellar disks (18 of 66) turned out to be there.

It is the sample by Erwin et al. (2008) that we took as a basis when we began our studies aimed at relating the stellar population properties in galactic nuclei to the shape of the outer disk brightness profile. This formulation of the problem provides a direct way of establishing the origin of the shape of the disk surface density profile. The point is that almost any galactic disk rearrangement, whether it is caused by internal factors (the instabilities giving rise to a bar) or external effects (the tidal effects from a neighbor, the swallowing of a companion, the squeezing of a cold gaseous disk by the pressure of an outer hot gaseous halo), results in an active gas inflow to the galactic center, which can lead to a starburst—in the nucleus itself or in the circumnuclear region. When

*E-mail: olga@sai.msu.su

the starburst ends, it leaves additional stars with an enhanced heavy-element abundance behind and, integrally, we will see a stellar population with an enhanced metallicity and a reduced age at this location. We have been finding such chemically decoupled nuclei at the centers of early-type galaxies since the pioneering paper by Sil'chenko et al. (1992). If the galactic disks were initially purely exponential and the two-tiered profiles appeared after the radial redistribution of matter through, for example, the swallowing of a companion ("minor merging"), then an imprint of this event in the form of a chemically decoupled, relatively young stellar nucleus should be left at the galactic center. Conversely, if the disk has retained an initially exponential profile since its formation, then it has underwent no violent rearrangements and there should be no secondary stellar population at the center. This has been the logic of the study being planned.

In this paper, we investigate the stellar population in the central regions of several galaxies with purely exponential (single-exponential) outer stellar disks. The sample by Erwin et al. (2008) contains 18 galaxies with single-exponential disks; 13 of them have the morphological type SB0–SB0/a. Previously, lenticular galaxies have already been actively attracted the attention of researchers who determined the stellar population parameters in the nucleus and the bulge by the method of two-dimensional spectroscopy. In particular, Sil'chenko (2006) provided the metallicities and mean stellar ages for the nuclei and bulges of NGC 2681, NGC 2787, and NGC 7743. The galaxy NGC 4245 was also studied in detail separately (Sil'chenko et al. 2009a). Now, it has become possible to add eight more objects to these galaxies for which we have found two-dimensional spectroscopy in the open Isaac Newton Group Archive of observational data at the La Palma Observatory. The galaxies were observed with the SAURON integral-field spectrograph on the 4-m William Herschel telescope—initially as part of the SAURON project (de Zeeuw et al. 2002) and, in the last two years, as part of the ATLAS^{3D} project. Cataloged characteristics of the galaxies investigated here are collected in Table 1.

SAURON: OBSERVATIONS AND DATA REDUCTION

The SAURON integral-field spectrograph is a "private" instrument and is used for observations on the 4.2-m William Herschel telescope on La Palma (Canary Islands) by an international team of researchers, including mostly representatives from France, the Netherlands, and Great Britain. A detailed (through without any key details) description of the spectrograph can be found in Bacon et al. (2001). Two large observational projects to investigate the kinematics and the stellar population in the central regions of nearby early-type galaxies have been implemented with this instrument: the SAURON project proper (1999–2002 observations, a sample of 72 galaxies) and the succeeding ATLAS^{3D} project (2007–2008 observations, more than 260 galaxies). The results of the former project have been published and are being published in a series of almost twenty papers. As regards the latter project, it has been announced that all observations have passed, but neither the preliminary results nor even the sample of galaxies itself have been published so far. However, according to the Observatory's rules, all raw observational data appear in the open Archive of the Cambridge Astronomical Data Center one year after the observations. Table 2 provides a summary of the details of the observations; some galaxies were observed in two "positions"—this means that the nucleus was set at one edge of the field of view in the first position and at the opposite edge in the second position. Maps of the double SAURON field of view with the galactic nucleus at the map center are obtained after the combination of the results of reducing the observations in "two positions."

The design principle of the SAURON spectrograph is based on the scheme of turning an entrance lenslet array through a small angle relative to the direction of dispersion called TIGER mode in the literature (Bacon et al. 1995); the second version of the MPFS integral-field spectrograph of the 6-m telescope (1994–1998) was also based on the same principle, which facilitated our work with the SAURON data. To make the arrangement of spectra on the detector ($4k \times 2k$ CCD) more compact, the interference filter in SAURON cuts out a narrow spectral range, about 4800–5350 Å, with both the filter transmission curve and the reverse dispersion changing (with beam tilt) over the field of view: in 1999–2002, it was within the range 1.11–1.21 Å per pixel; in 2007, the dispersion variations decreased noticeably after the replacement of the optics; now, this is 1.16–1.17 Å. The working field of view of the spectrograph is 44×38 spatial elements (spaxels) at a $0''.94$ scale per spaxel (per lenslet). The sky is exposed simultaneously with the object on the same CCD detector, on its extreme pixels, and it is taken at a mere $1'.7$ from the center of the object being studied. For large galaxies, this means that the outer galactic regions are exposed instead of the sky. We retrieved the data for the eight galaxies of interest to us that were observed during both projects from 2001 to 2008 (a list of exposure parameters is given in Table 2) from the open ING (Isaac Newton Group) Archive of the

Table 1. Global parameters of the galaxies being studied

Name	NGC 4267	NGC 4340	NGC 4477	NGC 4596	NGC 4643	NGC 4754	NGC 7743	IC 676
Type (NED[1])	SB(s)0−	SB(r)0+	SB(s)0:	SB(r)0+	SB(rs)0/a	SB(r)0−	(R)SB(s)0+	(R)SB(r)0+
$D(0)$, ′ (RC3[2])	3.2	3.4	3.7	3.8	3.1	4.2	3.0	2.4
B_T^0 (RC3)	11.77	12.01	11.30	11.50	11.54	11.33	12.16	12.70
M_B (LEDA[3])	−19.3	−18.9	−20.5	−20.9	−19.9	−20.2	−19.9	−18.2
$(B-V)_T^0$ (RC3)	0.91	0.91	0.94	0.92	0.93	0.90	0.84	–
V_r, km s^{-1} (NED)	1009	950	1355	1870	1335	1347	1710	1453
Distance[4], Mpc	16.8	16.8	16.8	16.8	25.7	16.8	24.4	–
Emission in nucleus? [5]	no	no	Sy2	Liner2::	H II/AGN2::	Sy2	H II	H II[10]
Environment (NOG[6])	Virgo cl.	Virgo cl.	Virgo cl.	Virgo cl.	field	Virgo cl.	field	group
Bar radius[7], arcsec	26	48	37	57	62	27	37	18
Earlier?	MPFS	–	–	–	–	long-slit[8]	MPFS[9]	–

[1] NASA/IPAC Extragalactic Database.
[2] de Vaucouleurs et al. (1991).
[3] Lyon–Meudon Extragalactic Database.
[4] Tully and Fisher (1988).
[5] Ho et al. (1997).
[6] Giuricin et al. (2000).
[7] Erwin (2005).
[8] Fisher et al. (1996).
[9] Sil'chenko (2006).
[10] Markaryan and Lipovetskii (1976).

Table 2. Spectroscopic observations of eight SB0 galaxies with SAURON

NGC	Date	$T_{\rm exp}$, min	$FWHM_*''$	PA(top), deg
NGC 4267, 1st position	Feb. 28, 2008	2 × 30	1.5	200
NGC 4267, 2nd position	Feb. 28/29, 2008	3 × 30	1.5	200
NGC 4340, 1st position	Jan. 14, 2008	2 × 30	1.6	190
NGC 4340, 2nd position	Jan. 14, 2008	2 × 30	1.6	190
NGC 4477	Mar. 25, 2001	4 × 30	1.7	209
NGC 4596	Apr. 19, 2002	4 × 30	1.8	264
NGC 4643	Apr. 14, 2007	2 × 30	2.5	60
NGC 4754, 1st position	Apr. 21, 2007	2 × 30	2.3	290
NGC 4754, 2nd position	Apr. 21, 2007	2 × 30	2.3	290
NGC 7743, 1st position	Aug. 14, 2007	3 × 30	2	−5
NGC 7743, 2nd position	Aug. 14, 2007	2 × 30	2	−5
IC 676	Mar. 6, 2008	2 × 30	1.1	188

Cambridge Astronomical Data Center together with the calibration exposures (bias, comparison, twilight-sky, and incandescent-lamp spectra). For the primary SAURON data reduction, we used the software package by Vlasyuk (1993) written for the MPFS data reduction and only slightly modified by its author to take into account the SAURON design peculiarities; accordingly, the reduction ideology was also the same as that when working with the data from the 1994–1998 MPFS version; it has already been described previously (Sil'chenko 2005). For one of the galaxies from our sample, NGC 4596, observed back in 2002 as part of the SAURON project, a completely reduced data cube was kindly provided to us for analysis by Dr. Falcon-Barroso.

To estimate the stellar population parameters in the galaxies being studied, we applied two independent methods—Lick indices (Worthey 1994) and direct fitting of the spectra with PEGASE.HR stellar population models (Le Borgne et al. 2004) by the NBursts technique (Chilingarian et al. 2007). The measurements of Lick indices allowed us to compare what is given by the SAURON data with published data. In computing the maps of the Lick Hβ, Mg*b*, and Fe5270 absorption-line indices (Worthey et al. 1994), we used an original software package in FORTRAN with the code by A. Vazdekis computing the Lick indices together with their statistical errors from the individual spectra of spaxels built in as its basic element. Since the SAURON spectral resolution, 4 Å, is higher than the standard Lick one, ∼8 Å, theoretically, the equivalent widths of the absorption lines must be exactly equal to the calculated indices. However, we did correct the "standard character" of our Lick indices based on the spectra of standard stars from the list by Worthey et al. (1994) observed in the same periods as the galaxies. The systematic deviations of our instrumental indices from the standard Lick ones do not exceed 0.2 Å and these small systematic corrections were applied to the measurements made for the galaxies. Based on the spectra of standard stars, we also studied what corrections should be applied to the indices being measured to take into account the broadening of lines in the galaxy spectra due to the stellar velocity dispersion. The spectrum of one giant star chosen in each set was convolved with a Gaussian of variable width following which the indices were remeasured from the broadened spectra and then compared with those measured from the "unspoilt" stellar spectrum. In this way, we established the dependence of the correction to the indices on σ_*; these dependences for each index were fitted by cubic and quartic polynomials. For a typical stellar velocity dispersion in giant lenticular galaxies, ∼200 km s^{-1}, the corrections to the indices for line broadening are 0.15 Å for Hβ, ∼0.3 Å for Mg*b*, and ∼0.6 Å for Fe5270; for a velocity dispersion of ∼100 km s^{-1}, these corrections are negligible.

The NBursts technique for direct fitting of the spectra with simple stellar population models provides a considerably higher accuracy of the stellar population parameters than the Lick indices due to a more efficient use of the spectroscopic information (Chilingarian 2009). Apart from the stellar population parameters (the age and mean metallicity), the technique allows the kinematic stellar population characteristics to be determined—the line-of-sight velocity, the velocity dispersion, and the deviation of the line-of-sight velocity distribution (LOSVD) from a purely Gaussian shape. The technique also allows the problems related to the presence of an emission component in the Hβ line and oxygen and nitrogen emission lines to be easily circumvented by eliminating small fragments of the spectral range from the fitting procedure. At the same time, this technique does not allow the [Mg/Fe] abundance ratio to be estimated, although the stellar population parameters being determined (the age and mean metallicity) were shown (Chilingarian et al. 2008) to be insensitive to [Mg/Fe] variations.

An additional step in the SAURON data reduction compared to the procedure described in Sil'chenko (2005) was the transformation of the data cubes to the Euro3D format.

CHEMICALLY DECOUPLED NUCLEI IN SB0 GALAXIES WITH EXPONENTIAL DISKS

Among the galaxies under consideration, IC 676 shows a purely emission spectrum with narrow lines and a weak stellar continuum over the entire SAURON field of view. We argue that intense star formation is currently going on at the center of this lenticular galaxy. The contribution to the integral spectrum from the ionized gas is too strong for the stellar population properties to be analyzed from the spectrum.

In the other seven galaxies, to trace the changes in stellar population characteristics with distance from the galactic center with the highest accuracy, we calculated the mean indices in rings from the constructed maps of Lick indices; the errors of these means estimated from the scatter of data points within the rings are everywhere less than 0.1 Å. However, this is the internal measurement accuracy; as regards the external accuracy, systematic errors can undoubtedly be present in the SAURON data. In particular, there is certainly stray light in the spectrograph whose level is unknown to us, because the owners of the spectrograph themselves deny its presence. In large

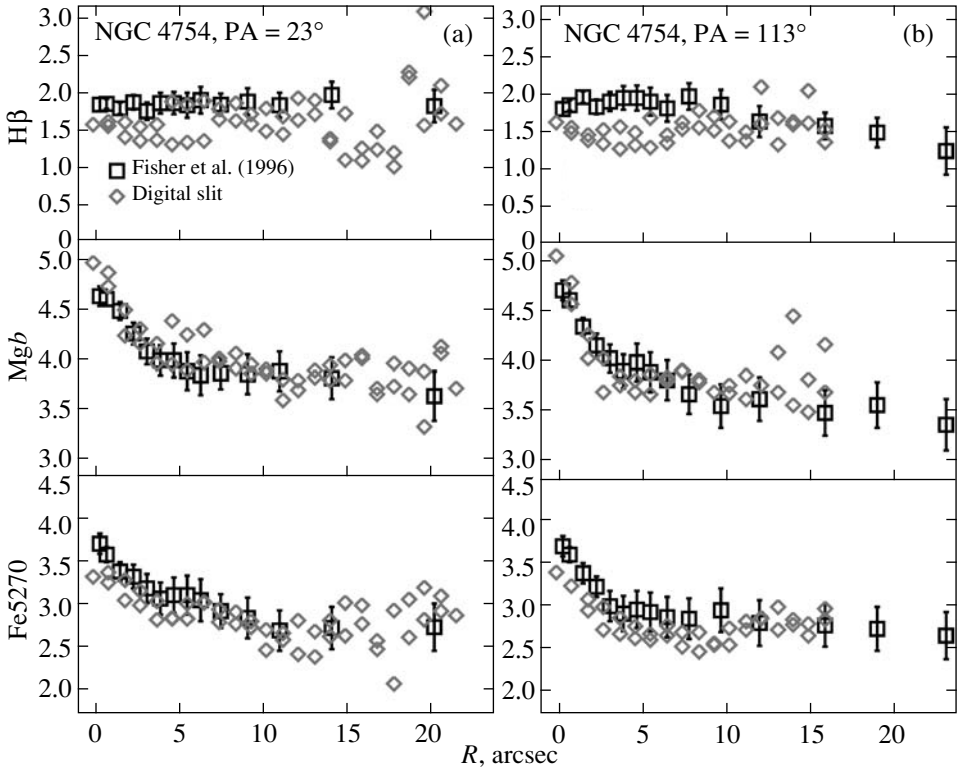

Fig. 1. Comparison of the Lick index profiles for various lines (in Å) along the major (a) and minor (b) axes for NGC 4754 based on the SAURON data (diamonds) and the long-slit spectroscopy by Fisher et al. (1996) (squares).

galaxies, there can also be background oversubtraction, because the sky background is measured less than 2 arcmin away from the galactic center. The former and latter effects should reduce and increase the absorption line equivalent widths, respectively.

As we indicated in Table 1, three galaxies from the list have already been observed earlier spectroscopically to measure the Lick indices along the radius. This can help us to get an idea of the possible level of systematic errors. In particular, the galaxy NGC 4754 was investigated by Fisher et al. (1996) with a long-slit spectrograph; the slit was set along the major and minor axes of the galaxy. We simulated long-slit observations by putting a digital mask on the two-dimensional maps of indices that we computed from the SAURON data. Our measurements are compared with the data from Fisher et al. (1996) along the major (PA = 23°) and minor (PA = 113°) axes in Fig. 1. The agreement is satisfactory, especially in the magnesium index whose line is in the middle of the SAURON spectral range. In the Hβ index, the SAURON data are probably systematically lower than the measurements from Fisher et al. (1996) by 0.2–0.4 Å. In Fig. 2, we compare the azimuthally averaged index profiles from the SAURON and MPFS data for NGC 4267 and NGC 7743. On the whole, the signal-to-noise ratio of the MPFS data is lower than that of the SAURON ones and the accuracy of the azimuthally averaged indices here is ~0.2 Å. However, we see excellent agreement between the measurements at the galactic centers (except the iron index in NGC 4267) and an underestimated magnesium index in the SAURON measurements is possible only at intermediate radii 2–5 arcsec. On the whole, all comparisons of Figs. 1 and 2 lead us to conclude that we see no statistically significant systematics at a level greater than 0.2–0.4 Å in the Lick indices measured from the SAURON data.

Figure 3 presents the radial age and metallicity profiles for seven galaxies from our sample. The profile construction process included several steps. First, the reduced data cubes in the Euro3D format were subjected to adaptive spatial binning using Voronoi tessellations (Cappellari and Copin 2003). During this procedure, we achieved a minimum specified signal-to-noise ratio in the spectrum in each bin, S/N from 60 to 100 per pixel at 5000 Å, depending on the object, through the summation of the signal in neighboring spaxels and, thus, degradation of the spatial resolution. Next, all spectra were fitted independently of one another with simple PEGASE.HR stellar population models using the NBursts technique. In fitting the spectra, we cut out short spectral

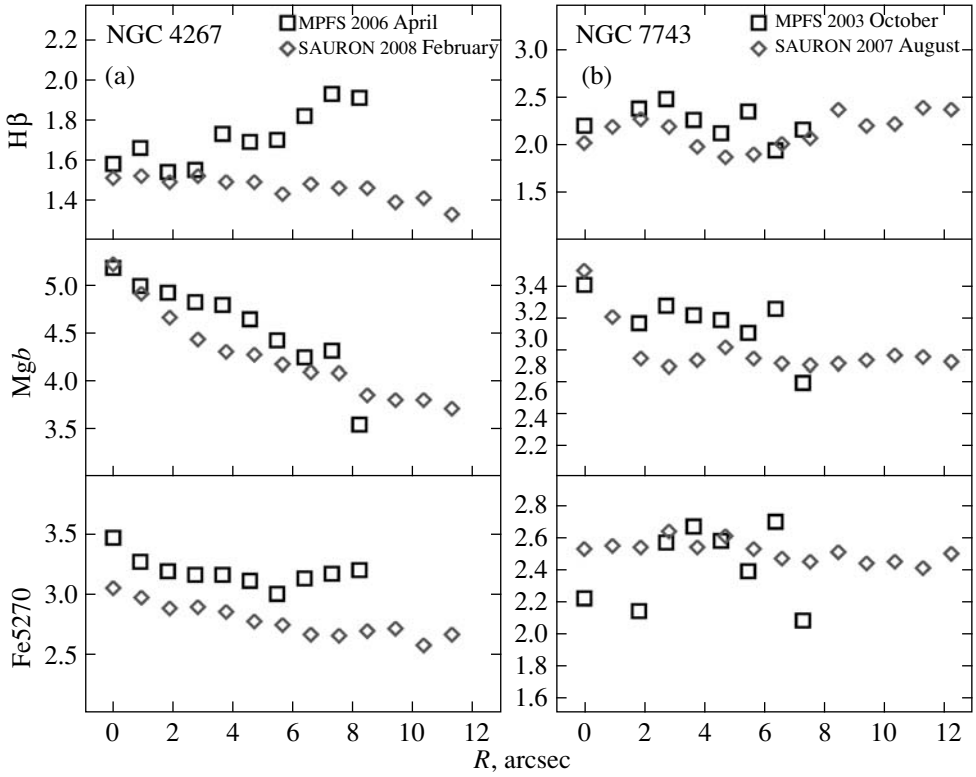

Fig. 2. Comparison of the azimuthally averaged Lick index profiles for various lines (in Å) from the SAURON (diamonds) and MPFS (squares) data for NGC 4267 (a) and NGC 7743 (b).

intervals around the Hβ, [O III], and [N I] emission lines in NGC 4477, NGC 4643, and NGC 7743. As a result, we obtained the kinematic and stellar population parameters for each bin. Subsequently, we reconstructed the two-dimensional maps of the distribution of these parameters in the galaxies from which the radial profiles presented in Fig. 3 were then constructed. The full two-dimensional maps of the kinematics and stellar population will be presented in a separate paper.

As we see from the presented age and metallicity profiles, for all galaxies in our sample at radii $r > 4 \ldots 7$ arcsec, the stellar population parameters change only slightly (for NGC 4267 and NGC 4477) or do not change at all; in contrast, the metallicity falls rather steeply with radius near the center. This shape of the radial distribution of the stellar population parameters is consistent with the view of chemically decoupled compact stellar nuclei: given the seeing, $1''.5$–$2''.5$, the contribution of the central source ceases to be dominant precisely at these distances from the center. We will assume that we see the galactic bulge outside the dominance of the radiation from the central stellar nucleus. The bulge metallicities lie within narrow ranges, -0.4 dex $<$ [Z/H] < -0.2 dex; the ages turn out to be old (10 Gyr or more for five galaxies, 6.7 Gyr for NGC 4340, and 2.2 Gyr for NGC 7743). The stellar population parameters for the nuclei differ significantly from those for the bulges in all cases. The mean metallicity [Z/H] in the nuclei exceeds that in the bulges by 0.3–0.5 dex. In three cases (NGC 4340, NGC 4643, and NGC 7743), the mean age of the stellar population in the nuclei also differs significantly from that in the bulges (in the direction of lower values). The youngest stellar population (1.2 Gyr) is observed in the nucleus of the Seyfert galaxy NGC 7743. It, along with the nucleus of NGC 4340, also exhibits the highest metallicity (+0.2 dex) among all galaxies from our sample.

The greatest metallicity difference between the nucleus and the bulge (+0.5 dex) is observed in galaxies where the stellar population of the nucleus is, on average, significantly younger than that of the bulge (NGC 4340, NGC 7743). This fact is consistent with the scenario in which the secondary starburst in the nucleus can have a different duration and/or a different efficiency. However, chemically decoupled stellar nuclei are present in all of the investigated galaxies with exponential outer stellar disks and, consequently, a secondary starburst of a particular duration and/or intensity took place.

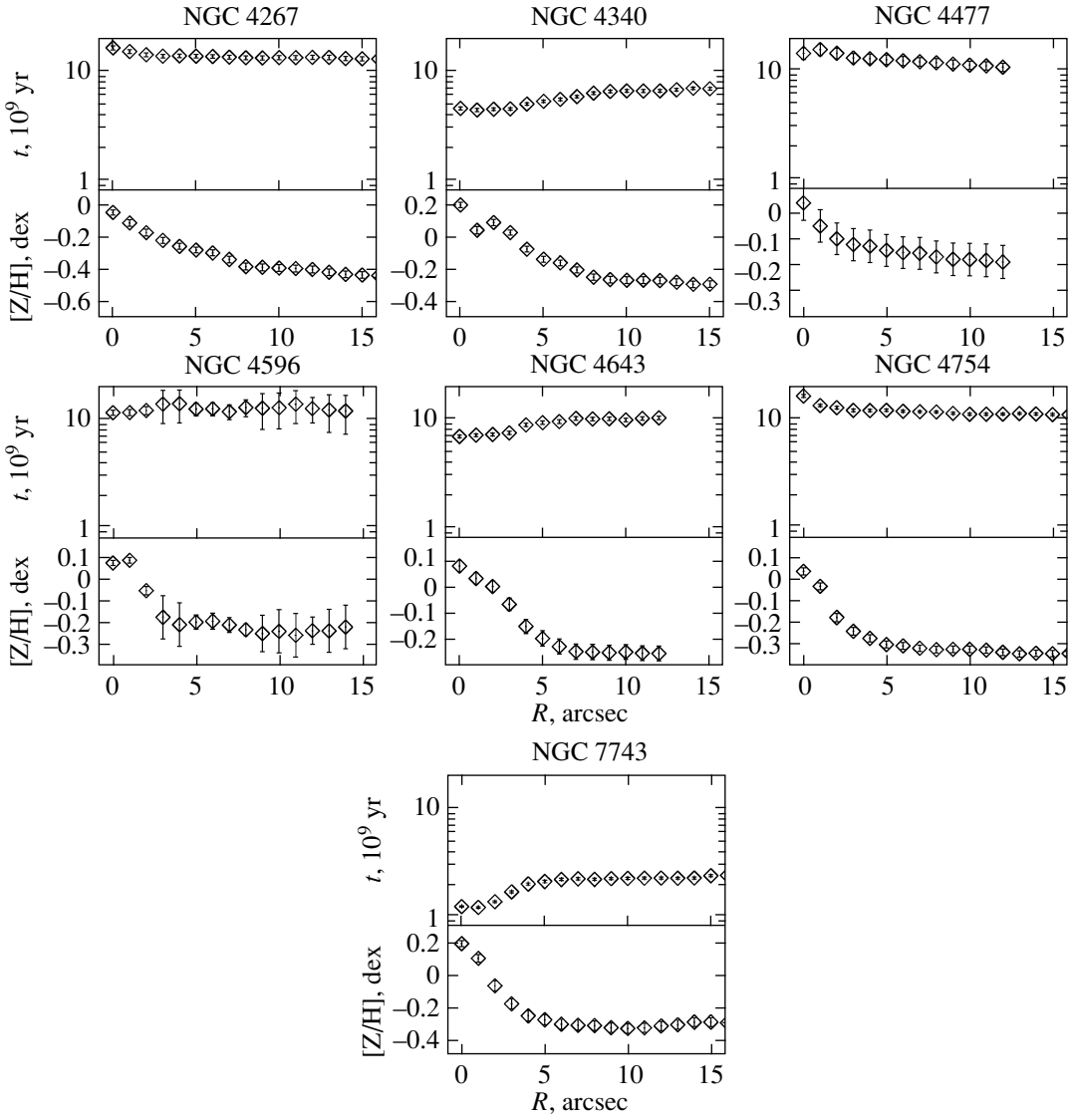

Fig. 3. Mean age and metallicity profiles of the stellar population at the centers of the galaxies studied obtained by averaging the two-dimensional distributions in rings.

DISCUSSION

In all seven galaxies with exponential outer stellar disks for which we analyzed the stellar population properties at the center based on the SAURON data, we detected chemically decoupled nuclei. The metallicity of the bulges beyond a radius of 5″ is always lower than the solar one, while the metallicity of the stellar nuclei, on the contrary, is always solar or higher; the metallicity difference between the nucleus and the bulge in all galaxies exceeds a factor of 2. We collected the stellar population characteristics of the chemically decoupled nuclei in Table 3. Note that the ages of the chemically decoupled nuclei are very different, from 1 to 15 Gyr. The age and metallicity maps for NGC 4596 obtained from the same SAURON data but using different evolutionary synthesis models were published by Peletier et al. (2007); these authors also pointed out a homogeneously old age of the stellar population over the entire SAURON field of view. An old age of the stellar nuclei in NGC 4477 and NGC 4596 was also obtained by Sarzi et al. (2005) from HST aperture spectroscopy. Finally, if we add the galaxies with exponential outer stellar disks investigated previously with the MPFS (Sil'chenko 2006) to the sample, then we will make sure that NGC 2681 has a very young nucleus, younger than 2 Gyr, while NGC 2787 has a very old nucleus, ∼15 Gyr. In this case, the metallicity of the chemically decoupled nuclei anticorrelates with their age (Fig 4). Everything appears as if the formation of the chemically decoupled nucleus began in all galaxies approximately at the same time and very

Table 3. Characteristics of the stellar population in the nuclei (columns 2–3) and bulges (columns 4–5) of seven SB0 galaxies

NGC	t_n, Gyr	$[Z/H]_n$, dex	t_b, Gyr	$[Z/H]_b$, dex
4267	15 ± 4	-0.05 ± 0.03	12 ± 3	-0.43 ± 0.05
4340	4.3 ± 0.5	$+0.19 \pm 0.04$	6.7 ± 0.6	-0.29 ± 0.05
4477	14 ± 3	$+0.05 \pm 0.08$	11 ± 3	-0.18 ± 0.10
4596	11 ± 1	$+0.09 \pm 0.03$	11 ± 4	-0.23 ± 0.10
4643	6.7 ± 0.5	$+0.09 \pm 0.03$	10 ± 1	-0.25 ± 0.04
4754	>15	$+0.05 \pm 0.03$	11 ± 1	-0.34 ± 0.04
7743	1.2 ± 0.1	$+0.19 \pm 0.05$	2.2 ± 0.1	-0.33 ± 0.05

long ago and ended differently—10 Gyr ago in some galaxies and almost "the other day" in other galaxies. In IC 676, this process continues to the present day. Since there are large-scale high-contrast bars in all galaxies "driving" the outer gas to the center, the duration of the central starburst can be determined by the initial store of gas. The influence of the environment should also be taken into account: the youngest chemically decoupled nuclei (and the most prominent emission) are in the galaxies that do not belong to the Virgo cluster. In the Virgo members NGC 4267, NGC 4596, and NGC 4754, there is little gas and the nuclei are relatively old. On the other hand, there is no gas in the Virgo member NGC 4340 either, while its nucleus is young, i.e., it lost its gas quite recently, less than 2 Gyr ago. In contrast, there is (accreted?) gas in NGC 4477, but its nucleus is old. It may well be that the main evolution in the lenticular galaxies of the cluster passed and finished before they joined Virgo.

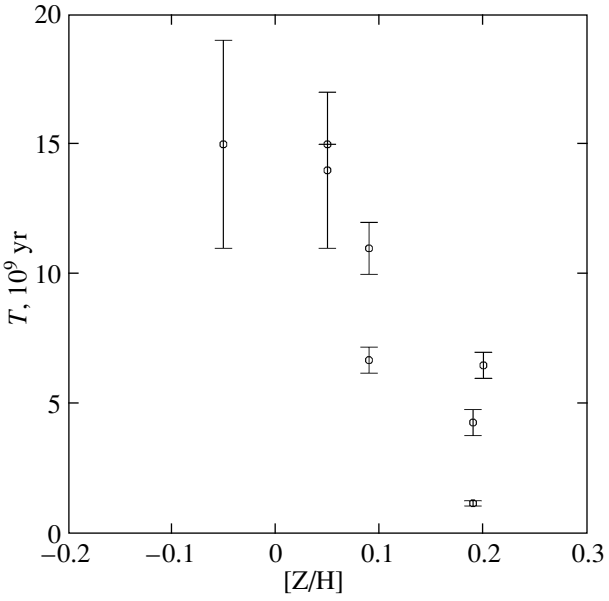

Fig. 4. Anticorrelation between the age and metallicity of the stellar population in the chemically decoupled nucleus of the investigated galaxies from the data of Table 3 with the addition of the results for NGC 4245 from Sil'chenko et al. (2009).

Thus, the chemically decoupled nuclei in galaxies with purely exponential outer stellar disks were formed in the process of long evolution; the term "secular evolution" is now commonly used for such slow evolution in the West (for a review, see Kormendy and Kennicutt, 2004). In this case, the gas flowed in along the radius to the center. However, this is the same process that leads to the gradual establishment of an exponential star surface density profile if the stars are formed on the time scales of the radial redistribution of gas (Lin and Pringle 1987)! The star formation time scales in the disks of spiral galaxies range from a few (2 or 3) Gyr for early types (Sa–Sb) to 10 Gyr for late types (Sc–Sd) (see, e.g., Charlot and Bruzual 1991). This range agrees with the range of ages for our chemically decoupled nuclei. Thus, if the precursors of lenticular galaxies were spiral galaxies of various types, then we will obtain this range of ages for the nuclei.

Let us now think what can distinguish the secular evolution of galaxies with exponential disks from that of galaxies with two-tiered disks. Among the galaxies with two-tiered disks in which we studied in detail the kinematics of their central regions, there is a high percentage of the detections of decoupled kinematics of the gaseous component with respect to the stellar one: both highly inclined inner rings or disks—NGC 6340 (Sil'chenko 2000, Chilingarian et al. 2009), NGC 524 (Sil'chenko 2000), NGC 7217 (Sil'chenko and Afanasiev 2000), NGC 615 (Sil'chenko et al. 2001), NGC 3599 (Sil'chenko et al. 2010), IC 1548 (Sil'chenko and Afanasiev 2008), and counterrotating fractions of both gas and stars directly in the large galactic disk—NGC 3626 (Ciri

et al. 1995; Sil'chenko et al. 2010), NGC 7742 (Sil'chenko and Moiseev 2006), NGC 7217 (Merrifield and Kuijken 1994; Sil'chenko and Afanasiev 2000), NGC 5631(Sil'chenko et al. 2009b), are encountered. We may have noticed nothing unusual in the kinematics only in the galaxies with two-tiered disks NGC 5533 (Sil'chenko et al. 1998) and NGC 7177 (Sil'chenko and Smirnova 2010). The presence of a small fraction of gas or stars with an intrinsic angular momentum unrelated to the galaxy's total angular momentum is usually explained by the swallowing of a small companion from an inclined orbit—the so-called minor merging. So far the only successful model for the construction of a two-tiered disk is also based on the idea of minor merging (see Younger et al. 2007). It is possibly the differences in the nature of the "trigger"of secular evolution that produce different shapes of the surface density profile for galactic disks: rearranging the gaseous disk on a short time scale, single-stage minor merging produces a two-tiered stellar disk, while a long-lived bar providing steady accretion of gas from the outer regions onto the center builds a regular exponential profile during several Gyr. Both mechanisms provoke starbursts in the nucleus but on different time scales. Chemically decoupled stellar nuclei will also appear in both cases.

ACKNOWLEDGMENTS

We used the observational data from the William Herschel telescope operated by the Royal Greenwich Observatory at the Spanish del Roque de los Muchachos Observatory of the Institute of Astrophysics of the Canary Islands; the data were retrieved from the open Isaac Newton Group Archive at the CASU Astronomical Data Center (Cambridge, Great Britain); we are also grateful to Dr. Jesus Falcon-Barroso, who provided the reduced SAURON data cube for NGC 4596. During our work, we relied on the means of the Lyon–Meudon Extragalactic Database (LEDA) provided by the LEDA team at the Lyon CRAL Observatory (France) and the NASA/IPAC database (NED) operated by the Jet Propulsion Laboratory of the California Institute of Technology under contract with NASA (USA). This work was supported by the Russian Foundation for Basic Research (project no. 07-02-00229a).

REFERENCES

1. R. Bacon, G. Adam, A. Baranne, et al., Astron. Astrophys. Suppl. Ser. **113**, 347 (1995).
2. R. Bacon, Y. Copin, G. Monnet, et al., Mon. Not. R. Astron. Soc. **326**, 23 (2001).
3. D. Le Borgne, B. Rocca-Volmerange, P. Prugniel, et al., Astron. Astrophys. **425**, 881 (2004).
4. M. Cappellari and Y. Copin, Mon. Not. R. Astron. Soc. **342**, 345 (2003).
5. S. Charlot and A. G. Bruzual, Astrophys. J. **367**, 126 (1991).
6. I. V. Chilingarian, P. Prugniel, O. K. Silchenko, and V. L. Afanasiev, Mon. Not. R. Astron. Soc. **376**, 1033 (2007).
7. I. V. Chilingarian, V. Cayatte, F. Durret, et al., Astron. Astrophys. **486**, 85 (2008).
8. I. V. Chilingarian, Mon. Not. R. Astron. Soc. **394**, 1229 (2009).
9. I. V. Chilingarian, A. P. Novikova, V. Cayatte, et al., Astron. Astrophys. **504**, 389 (2009).
10. D. K. Churches, A. H. Nelson, and M. G. Edmunds, Mon. Not. R. Astron. Soc. **327**, 610 (2001).
11. R. Ciri, D. Bettoni, and G. Galletta, Nature **375**, 661 (1995).
12. C. J. Clarke, Mon. Not. R. Astron. Soc. **238**, 283 (1989).
13. P. Erwin, Mon. Not. R. Astron. Soc. **364**, 283 (2005).
14. P. Erwin, M. Pohlen, and J. E. Beckman, Astron. J. **135**, 20 (2008).
15. D. Fisher, M. Franx, and G. Illingworth, Astrophys. J. **459**, 110 (1996).
16. K. C. Freeman, Astrophys. J. **160**, 811 (1970).
17. G. Giuricin, Ch. Marinoni, L. Ceriani, and A. Pisani, Astrophys. J. **543**, 178 (2000).
18. L. C. Ho, A. V. Filippenko, and W. L. W. Sargent, Astrophys. J. Suppl. Ser. **112**, 315 (1997).
19. J. Kormendy and R. C. Kennicutt, Jr., Ann. Rev. Astron. Astrophys. **42**, 603 (2004).
20. D. N. C. Lin and J. E. Pringle, Astrophys. J. **320**, L87 (1987).
21. B. E. Markaryan and V. A. Lipovetskii, Astrofizika **12**, 389 (1976).
22. M. R. Merrifield and K. Kuijken, Astrophys. J. **432**, 575 (1994).
23. R. F. Peletier, J. Falcón-Barroso, R. Bacon, et al., Mon. Not. R. Astron. Soc. **379**, 445 (2007).
24. M. Pohlen and I. Trujillo, Astron. Astrophys. **454**, 759 (2006).
25. M. Sarzi, H.-W. Rix, J. C. Shields, et al., Astrophys. J. **628**, 169 (2005).
26. O. K. Sil'chenko, Astron. J. **120**, 741 (2000).
27. O. K. Sil'chenko, Astrophys. J. **641**, 229 (2006).
28. O. K. Sil'chenko and V. L. Afanasiev, Astron. Astrophys. **364**, 479 (2000).
29. O. K. Sil'chenko and V. L. Afanasiev, Astron. Zh. **85**, 972 (2008) [Astron. Rep. **52**, 875 (2008)].
30. O. K. Sil'chenko and A. V. Moiseev, Astron. J. **131**, 1336 (2006).
31. O. K. Sil'chenko and A. A. Smirnova, Pis'ma Astron. Zh. **36**, 334 (2010) [Astron. Lett. **36**, 319 (2010)].
32. O. K. Sil'chenko, V. L. Afanasiev, and V. V. Vlasyuk, Astron. Zh. **69**, 1121 (1992) [Sov. Astron. **36**, 577 (1992)].
33. O. K. Sil'chenko, A. N. Burenkov, and V. V. Vlasyuk, New Astron. **3**, 15 (1998).
34. O. K. Sil'chenko, V V. Vlasyuk, and F. Alvarado, Astron. J. **121**, 2499 (2001).

35. O. K. Sil'chenko, Pis'ma Astron. Zh. **31**, 250 (2005) [Astron. Lett. **31**, 227 (2005)].
36. O. K. Sil'chenko, I. V. Chilingaryan, and V. L. Afanasiev, Pis'ma Astron. Zh. **35**, 87 (2009a) [Astron. Lett. **35**, 75 (2009)].
37. O. K. Sil'chenko, A. V. Moiseev, and V. L. Afanasiev, Astrophys. J. **694**, 1550 (2009b).
38. O. K. Sil'chenko, A. V. Moiseev, and A. P. Shulga, Astron. J. **140**, 1462 (2010).
39. A. D. Slyz, J. E. Devriendt, J. Silk, and A. Burkert, Mon. Not. R. Astron. Soc. **333**, 894 (2002).
40. R. B. Tully and J. R. Fisher, *Catalog of Nearby Galaxies* (Cambridge Univ., Cambridge, UK, 1988).
41. G. de Vaucouleurs, Handbook de Physique **53**, 311 (1959).
42. G. de Vaucouleurs, A. de Vaucouleurs, H. G. Corwin, Jr., et al., *The 3rd Reference Catalogue of Bright Galaxies* (Springer, Berlin, Heidelberg, New York, 1991), p. 2069.
43. V. V. Vlasyuk, Astrofiz. Issled. (Izv. SAO RAN) **36**, 107 (1993).
44. G. Worthey, Astrophys. J. Suppl. Ser. **95**, 107 (1994).
45. G. Worthey, S. M. Faber, J. J. Gonzalez, and D. Burstein, Astrophys. J. Suppl. Ser. **94**, 687 (1994).
46. J. D. Younger, T. J. Cox, A. C. Seth, and L. Hernquist, Astrophys. J. **670**, 269 (2007).
47. P. T. de Zeeuw, M. Bureau, E. Emsellem, et al., Mon. Not. R. Astron. Soc. **329**, 513 (2002).

Translated by V. Astakhov